International Journal of Robotics and Control Systems
Vol. 5, No. 1, 2025, pp. 348-365
ISSN 2775-2658
http://pubs2.ascee.org/index.php/ijrcs

Optimal Controller Design of Crowbar System Using Class Topper Optimization: Towards Alleviating Wind-Driven DFIGs Under Nonstandard Voltages

Mohamed F. Elnaggar [a,1,*]

[a] Department of Electrical Engineering, College of Engineering, Prince Sattam Bin Abdulaziz University, Al-Kharj 11942, Saudi Arabia
[1] mfelnaggar@yahoo.com
* Corresponding Author

ARTICLE INFO

Article history
Received October 31, 2024
Revised December 28, 2024
Accepted January 09, 2025

Keywords
Grid Faults;
Class Topper Optimization;
Power Quality;
DFIG;
Wind Energy

ABSTRACT

Increased integration of doubly fed induction wind generators (DFIWG), power sector deregulation, rising energy demands, and technological breakthroughs are all contributing to the rapid advancement of modern energy infrastructure. These advancements, nevertheless, pose serious challenges to maintaining fault ride-through capability (FRTC) in DFIWG. Thus, this work proposes a novel FRTC enhancement method that uses a crowbar system with a class topper optimization (CTO) based control technique. The crowbar system and DFIWG are integrated with the investigated system to achieve FRTC, reduce injected harmonic distortion, and maintain the DC link voltage (DCLV) below the permitted level. Additionally, the system has a DCLV control system that uses a CTO-PI controller to maintain an enclosure DCLV, which enhances crowbar performance. The findings demonstrated that when a CTO-based controller is employed, the DFIWG system reacts slightly better to angular speed, active and reactive power, DCLV, and generator speed. The MATLAB/Simulink scenarios used to test the suggested system show that it can achieve FRTC and allow for a high penetration potential of DFIWG.

1. Introduction

Electrical energy is of interest to businesses, governments, and research institutes worldwide, and there is an ongoing debate over which industrialized and developing countries should prioritize certain generation methods. For example, reducing pollutant emissions from conventional power plants that use fossil fuels like coal and oil is one of the top concerns for developed countries [1]-[3]. Following a string of global events, such as the devastating tsunami disaster in Japan that destroyed nuclear reactors, which many of these nations once supported, nuclear reactors are now viewed as possible risks [4]-[6].

To overcome the financial and geopolitical barriers that prevent them from building nuclear reactors, developing countries are searching for solutions to lower the high prices of conventional power. Therefore, renewable energy (RE) provides a solution that benefits all parties. Though at varying rates and capacities, the well-known RE sources—solar, wind, biomass, geothermal, and tidal—are widely used worldwide. However, the most often used systems at the moment are those

that generate electricity using solar and wind power. Over the past decade, wind power capacity has increased at a rate of over 20% annually in both Europe and the US, according to statistics. That more than 20% of the energy produced worldwide will come from wind power over the next 20 years [7]-[10].

Similar to this, the D-government and other pertinent parties have created a plan to increase the share of wind energy (WE) in the Danish power system (DPS) to 50% of the grid's total capacity. However, the most significant obstacles to the general use of solar energy (SE) production are the specific requirements for its manufacture, including the large surfaces needed and the sophisticated and expensive processes required to create SE cells [11]-[13]. Unlike solar energy, which is only available during specific seasons of the year, WE are available year-round. Many businesses provide a variety of wind turbines (WTs), with varying models offering competitive pricing and varying levels of efficiency. However, there are also well-known and intricate WTs with intricate controls that demonstrate the ongoing work needed to achieve the highest levels of energy harvesting efficiency and maintain PS stability [14]-[16].

Several approaches with a variety of technical techniques have been presented in this field to boost the FRT capabilities (FRTCs) of DFIWGs [17]-[20]. They are divided into two main categories: two types of methods: (1) passive (PMs) and (2) active (AMs). PMs include the following: pitch regulator [21], FACTS [22], fault current limiters [23], SDR [24], additional hardware systems with traditional crowbar protection circuits [9], [25], [26], and storage system [27]-[29]. In contrast, suitable converter regulates have been used in AMs to improve the FRTC of DFIWG in lieu of employing expensive tools, as in the case of the feed-forward transient current control scheme for RSC of DFIWG that was suggested in [30], alongside a traditional crowbar circuit. The drawbacks of PM are that the installation for extra tools results in higher costs. For providing reliable voltage disruption ride through with continuous power preparation, a common grid edge converter with a series GSC was utilized [31]. likewise, it has been shown to be more successful to satisfy the initial grid code needs by using exclusively conventional flux-oriented vector control approaches for converter regulation [32]. Even though these control methods are straightforward, they are ineffective in maintaining the FRTC of DFIWG when the grid experiences significant voltage sags because they are extremely reactive to the machine's parameters [33], [34]. Regulators have been made to guarantee the FRTC under voltage dips with the support of intelligent controllers (fuzzy, and sliding mode) [35] and it was superior to formerly PI controllers. In [36], a linear controller was developed to handle the after-fault scenario. However, it is exceedingly difficult to set up these techniques in a complicated back-to-back converter based DFIWG system because of their mathematical and computational complexity. Due to their ease of use and control, modified crowbar protection circuits are still preferred [37], [38]. As a result, this work aims to develop crowbar system with the GSA. In addition, three scenarios in four cases are studied to prove the effectiveness of the proposed method. Table 1 shows a comparison between the suggested work in DFIWG and earlier publications.

2. Description, and Control of the Studied System Components

Additional features enable DFIWGs to operate at somewhat different speeds than their intrinsic synchronous pace. Large DFIWGs benefit from this since wind speeds (v_w) can change quickly. When a gust hits a WT, its blades try to accelerate, but synchronous generators can't since they're synchronized to the grid's speed. The electrical grid pushing back puts a lot of strain on the hub, gearbox, and generator. This wears down and damages the mechanism. If the WT is allowed to accelerate immediately after being struck by a gust, the strains are lessened and the energy of the wind gust is converted into useful electricity [47]-[49].

2.1. Power Conversion of DFIWG

While the stator winding of the DFIWG is directly connected to the grid, the rotor windings are connected to a power converter. The grid energizes the stator windings to generate the stator magnetic

field. The converter energizes the rotor windings, creating a magnetic rotor field. Torque is the result of the interaction between the rotor and stator magnetic fields. The amount of torque generated depends on the relative angular displacement and the total intensity of the two magnetic fields. The stator's field is dependent on the grid voltage due to its direct connection to the grid, and its rotation is dependent on the grid frequency and syn., speed because the stator flow might be considered a constant. Grid voltage can be thought of as a relatively constant in steady-state operation, where the power converter directly controls the rotation of the rotor flux. Therefore, adjusting the magnitude and angle of the rotor current to the stator flux will have a direct impact on the torque generated in the DFIWG. It is feasible to determine the angular location and stator flux of the magnitude by applying a stator voltage that is in line with the grid voltage and phase and controlling the rotor current such that it is perpendicular to the stator flux and sufficiently large to supply the required torque.

Table 1. Comparison of the proposed work with previously published works

Refs.	Remarks
[39]	When a failure happens rapidly, applied feed-forward current regulation lowers the transient current in the rotor circuit.
[40]	Using a combined vector and direct power controller, the stator and rotor surges were reduced, and Q was rapidly fed during VDs.
[41]	The addition of a modified adaptive control architecture to the standard vector control system proved successful in mitigating sensor malfunctions and parameter fluctuations while ensuring acceptable performance during faults or wind speed situations.
[42]	At the POCC, a nonlinear SMC-based FCL was connected to enhance system performance. The results indicated that SMC functions effectively with nonlinear dynamics and unforeseen VD levels.
[43]	Depending on the VD level, the dynamic adaptive multi-cell FCL topology provides a variable VD compensation mechanism and greatly enhances system performance when coupled at the POCC. The effectiveness of the proposed method was confirmed by comparison evaluation with the single-cell FCL.
[44]	When the FLC, H∞, and PI controllers were compared for performance, H∞ performed the best. The FL-H∞ and the PI&PID-Filter derivative-H∞ are mixed controllers that provide improved performance and lower harmonics.
[45]	The accuracy of the three controllers that offered the lowest tracking error—SM, PI, and advanced backstepping (AB)—was examined and evaluated. Target monitoring, current waveform compatibility, rapid response time, and resilience were among the advantages of the ABC.
[46]	The MPC system was more effective than the PI type and was used to optimize the amount of wind energy harvested even in situations when the wind speed is unpredictable or the WT is uncertain.
Current study	The FRTC is achieved with the CTO-PI control for the crowbar. Voltage swell and dip are taken into account in this investigation. THD analysis is also taken into consideration to demonstrate the function of the suggested approach. The improved controller operates smoothly and responds quickly.

2.2. Control and Operation of Rotor Side Converter (RSC)

The torque production of the DFIWG is controlled by directly adjusting the rotor current of the RSC as seen in Fig. 1. By providing the rotor windings with a voltage equal to the intended current, the RSC achieves this. Variable RSC runs of v_w at different frequencies are necessary. The output power of the DFIWG can be controlled by the torque, speed, or active power controls on the RSC. The WTs' power speed characteristic curve is followed by adjusting this output power. Essentially, the v_w determines how much power can be extracted. PI controllers are typically used to control torque, speed, or power to their reference values. The output of any controller used is the reference rotor current required to deliver the required torque, power, or speed. The rotor voltage reference is the controller output, and the rotor current error is introduced from the reference value using the PI's inner control loop. Reactive power production by the DFIWG can also be controlled by the rotor current.

2.3. Control and Operation of Grid Side Converter (GSC)

The GSC controls the DCLV between two converters as seen in Fig. 1. GSC on the outer loop regulates the DCLV in an attempt to keep it within the acceptable limit. The PI inner control loop regulates the GSC current. The GSC typically sets Qgc = 0 and maximizes active power output. The

GSC must supply electricity at a steady frequency that corresponds to the grid frequency because of its direct grid connection.

2.4. Mathematical Modelling of DFIWG

A popular setup for capturing wind energy is DFIWG, which enables variable speed operation. The WT's mechanical power is determined by.

$$P_m = \frac{1}{2}\rho A C_p(\lambda,\beta)v_w^3 \tag{1}$$

where, ρ, A, $C_p(\lambda,\beta)$, λ, β are the air density, swept area, power coefficient, tip speed ratio, and blade pitch angle, respectively.

The λ is well-defined as,

$$\lambda = \frac{\omega_t R}{v_w} \tag{2}$$

where, R, and ω_t are the radius of rotor blades and the rotational speed of WT.

The dynamic model of the DFIWG in the d-q reference frame is given by following Eqs.

The stator voltage Eqs., are:

$$v_{ds} = R_s i_{ds} + \frac{d\psi_{ds}}{dt}\omega_s\psi_{qs} \tag{3}$$

$$v_{qs} = R_s i_{qs} + \frac{d\psi_{qs}}{dt}\omega_s\psi_{ds} \tag{4}$$

The rotor voltage Eqs., are:

$$v_{dr} = R_r i_{dr} + \frac{d\psi_{dr}}{dt}(\omega_s - \omega_r)\psi_{qr} \tag{5}$$

$$v_{qr} = R_r i_{qr} + \frac{d\psi_{qr}}{dt}(\omega_s - \omega_r)\psi_{dr} \tag{6}$$

where, (v_{ds} and v_{qs}), (v_{dr} and v_{qr}), (i_{ds} and i_{qs}), (i_{dr} and i_{qr}), ($\psi_{ds},\psi_{qs},\psi_{dr},\psi_{qr}$), and ($R_s$, and R_r) are the stator voltages, rotor voltages, stator currents, rotor currents, flux linkages (FL), and stator and rotor resistance, respectively.

The FL Eqs., are:

$$\psi_{ds} = L_s i_{ds} + L_m i_{dr} \tag{7}$$

$$\psi_{qs} = L_s i_{qs} + L_m i_{qr} \tag{8}$$

$$\psi_{dr} = L_r i_{dr} + L_m i_{ds} \tag{9}$$

$$\psi_{qr} = L_r i_{qr} + L_m i_{qs} \tag{10}$$

where, (L_s and L_r), L_m, ω_s, and ω_r labels the stator and rotor inductance, mutual inductance, synchronous angular velocity (AV), and rotor AV, respectively.

2.5. Modelling of Crowbar

The crowbar action can often be represented as in (16). The parameters for each of the subsequent equations are explained in detail [50]-[52].

$$V_C = F_S\, R_C\, I_C \tag{11}$$

$$T_r{}^{SC} = \left(\frac{L_r{}^{SC}}{R_r + R_{\tau c}}\right) \tag{12}$$

$$I_r{}^{max} = \left(\frac{V_r{}^{max}}{\sqrt{(X_r{}^{sc})^2 + (R_{\tau c})^2}}\right) \tag{13}$$

$$R_{\tau c} < \left(\frac{\sqrt{2}\, X_{rs}{}^{sc}\, V_r{}^{max}}{\sqrt{3.2\,(V_s)^2 + 2(V_r{}^{max})^2}}\right) \tag{14}$$

$$V_r = k\, m\, V_{DC}\,, and\ k = \left(\frac{1}{\sqrt{3}}\right)\frac{V_{DC}{}^{b}}{V_r{}^{b}} \tag{15}$$

$$V_r{}^{max} = IR_{DC} - V_{DC} = 0 \tag{16}$$

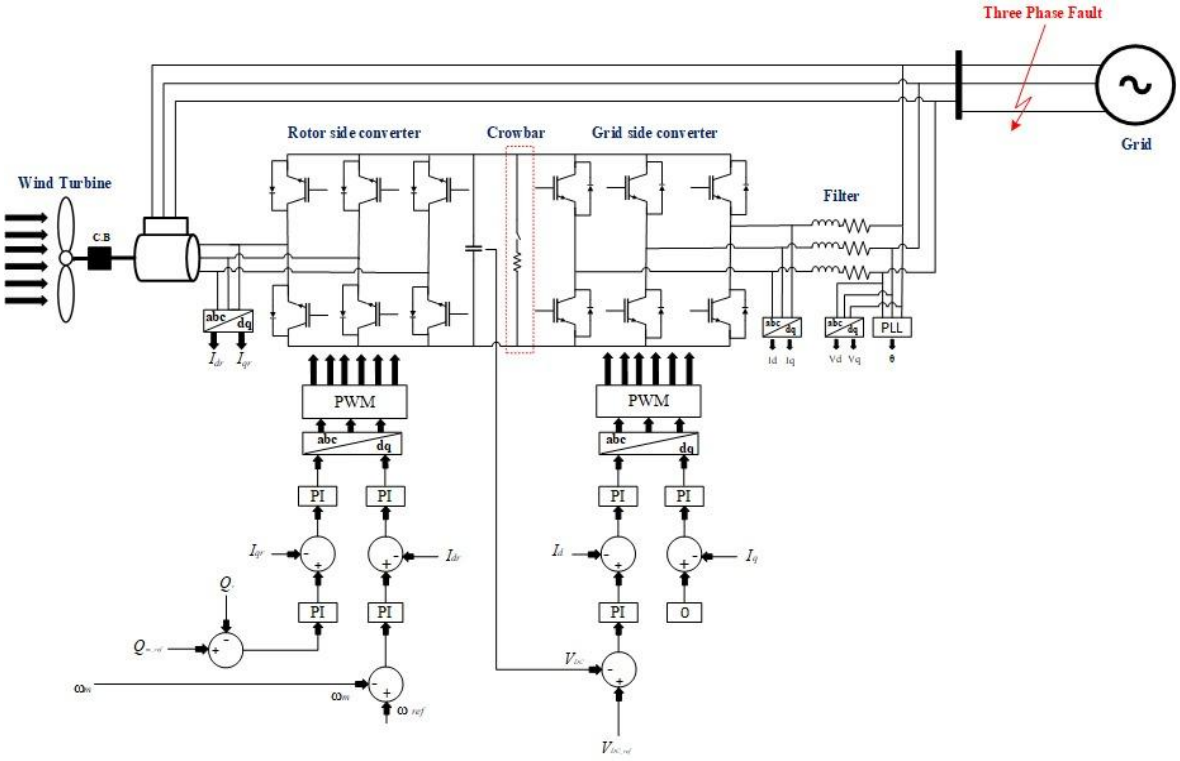

Fig. 1. Grid connected DFIWG with its control system

3. Applications of Class Topper Optimization (CTO) for Crowbar

3.1. Investigated CTO

Based on the academic behavior of students who aim to be the best in their class, the CTO [26] is a population-based meta-heuristic optimization. To improve student performance, the CTO primarily takes use of the competitive and cooperative dynamics that are seen among them and converts these ideas into a strong optimization plan. The fundamental concept of CTO is to model how students learn as they move through several phases of development, picking up tips from their classmates and high achievers before arriving at the best possible solution. The possible solutions in this method are represented by the students, who are further subdivided into multiple parts that essentially reflect the population subset. Students compete in each section to learn from the section

topper (ST), who is the best student in that section, to enhance their performance. The class topper (CT) sets the standard for other solutions to follow and build upon, and the STs learn from them. Section level and student level are the two primary stages of the learning mechanism in the CTO algorithm.

(A) Student (S) Level: Each S learns from the ST to upgrade their status at the S level. A learning factor also directs this update, repositioning the S according to the difference between its current position and that of the ST. Through imitation of the finest solutions in their local and global settings, this hierarchical learning process guarantees that every S gradually improves their performance.

(B) Section Level (SL): STs learn from CTs at the SL. This process is mathematically modeled by adjusting the ST's position according to the difference between its current position and the position of the CT, scaled by a learning factor. Randomness is incorporated into this learning element to maintain diversity and avoid local optima from forming too soon.

Through a sequence of iterations known as exams, the CTO functions. Ss use a predetermined fitness function to assess their success on each exam (E). The fitness function, which is comparable to academic scores, measures the quality of the answer. The S's ST learning process is mathematically designed as follows:

$$I^{(S,E+1)} = I_{WF} \times I^{(S,E)} + c \times n_2 \times \left(ST_{pi}^{(SE,E)} - S_{pi}^{(S,E)}\right) \tag{17}$$

$$ST_{pi}^{(S,E+1)} = S_{pi}^{(S,E)} + I^{(S,E+1)} \tag{18}$$

where, $I^{(S,E)}$ signifies upgrading in the information of S in E. This signifies the current knowledge level (CKL) of the S earlier the erudition repetition. Furthermore, $I^{(S,E+1)}$ embody the rationalized data neck and neck, I_{WF} epitomizes the inertia weight factor (WF), c is the acceleration coefficient, $S_{pi}^{(S,E)}$ is the present S fitness value and $ST_{pi}^{(SE,E)}$ is the place of the best-performing S in the section. The n_2 is the uniform random number that introduces a stochastic element to the learning process (LP). The LP of ST from CT is mathematically devised as,

$$I_1{}^{(SE,E+1)} = I_{WF} \times I^{(SE,E)} + c \times n_1 \times \left(CT_{pi}^{(E)} - S_{pi}^{(SE,E)}\right) \tag{19}$$

$$ST_{pi}^{(SE,E+1)} = ST_{pi}^{(SE,E)} + I_1{}^{(SE,E+1)} \tag{20}$$

where, $I^{(SE,E)}$ specifies CLV of ST in section SE, $I_1{}^{(SE,E+1)}$ represents updated KL of ST, $CT_{pi}^{(E)}$ defines the recital index (PI) of CT during check, $S_{pi}^{(SE,E)}$ indicates PI of ST and $ST_{pi}^{(SE,E+1)}$ is the rationalized PI of ST in SE during inspection E. The I_{WF} reductions linearly and improves convergence distinguishing,

$$I_{WF}^{E} = I_{WF_{max}} - \left(\frac{I_{WF_{max}} - I_{WF_{min}}}{E_{max}} \times E\right) \tag{21}$$

Here, I_{WF}^{E} is the inertial WF at examination E and E_{max} is the maximum number of Es. The $I_{WF_{max}}$ and $I_{WF_{min}}$ are the max. and min. I_{WF}. The CTO iterates through these LPs until it converges to an optimal solution or reaches a predefined number of examinations. The continuous interaction between students, section toppers, and the class topper fosters a dynamic environment where solutions evolve towards global optima.

The efficiency of CTO has been proven in some optimization problems, such as data clustering, load frequency control in power systems, and other intricate real-world situations. Its hierarchical learning mechanism and capacity to strike a balance between exploration and exploitation make it an effective tool for high-dimensional and multimodal optimization problems.

3.2. Applications of CTO-Based PI Controller

In this work, the CTO is used to adaptively tune the PI controller's parameters, which control the DCLV of the DFIWG. For the DFIWG to operate effectively, a stable DCLV must be maintained. Therefore, the PI controller is optimized with CTO to achieve exact voltage control. The technique iteratively refines the K_p and K_i Parameters, which are initially assigned random values, minimize the integral time absolute error (ITAE), which acts as a fitness function. In the optimization process, the performance of the PI controller is assessed using the existing parameters. The parameters are then updated based on the best-performing solutions, and the process is repeated until the maximum number of iterations or optimal parameters are determined. The DCLV is then regulated by the PI controller using the optimal K_p and K_i values. To keep the voltage level at the desired level, it modifies the control signals sent to the crowbar's switching components. By ensuring that the controller operates at its best across a range of operating situations, this adaptive tuning process improves system stability and dynamic response. Fig. 2 shows the CTO-PI controller flowchart, and Fig. 3 shows the DCLV control structure using CTO-PI. The following is the definition of the objective function (OF) for PI controller parameter optimization using the CTO:

$$OF = \int_0^T t \left| V_{dc(ref)} - V_{dc(act)+P_{(ref)}-P_{(act)+}} \right| dt \tag{22}$$

To begin, the CTO simulates a classroom setting in which every student stands for a possible solution set, in this case, a pair of PI controller settings. All students are given beginning values for these parameters at random to start the process. There are groups of Ss in each of the parts that make up the classroom. The fitness function—in this case, the ITAE—is used to determine the ST in each section. The CT is determined by taking the best S in every sector. Throughout the optimization process, the ITAE—which is the integral of the product of time and absolute error between reference and real DCLV—is used to assess each S's performance. Students learn from both the CT and the ST to keep up with current information. The PI parameters for these LPs are adjusted to match the toppers' values.

To ensure diversity and prevent local minima, the improvement in each S's parameters is mathematically stated as a weighted sum of their current parameters and the difference between their own and the topper's parameters, scaled by random factors. Throughout multiple cycles, the CTO continuously updates and improves the PI settings for every S. Every iteration also updates the CT and STs in light of the new performances. Until the stopping criterion—either the maximum number of iterations or another criterion—is satisfied, this iterative process continues. To control DCLV in the DFIWG system, the PI controller uses the final CT parameters, which are regarded as the ideal PI parameters.

3.3. Impacts of CTO-Based PI Controller on DFIWG

The responsiveness of DFIWG is negatively affected by grid failures. Increased generator speeds, electromagnetic torque oscillations, overcurrents, overvoltage at the DCLV, and a drop in the output power are the outcomes of these issues [53], [54]. Because electricity converters are the most expensive component of the DFIWG and are susceptible to damage, researchers have developed hardware and software solutions to shield DFIWG from the aforementioned negative outcomes. Important considerations for the converters include supply safety and durability, effectiveness, price, size, safeguarding, regulation of P and Q facilitating technologies, and FRTC [55].

The crowbar protects the DFIWG and improves system responsiveness in the event of a grid outage. DFIWG can weather the fault and maintain energy even in the case of a grid failure by employing a crowbar. The values of Ki and Kp for DFIWG are 0.06449. The data being monitored and directed to are the controller's inputs, and its output determines how to operate the system while considering the sawtooth signal. The recommended crowbar control method for the DFIWG under study is depicted in Fig. 3.

4. Results and Discussions

Dynamic performance improvement of DFIWG under different conditions is discussed in this work to show the role of the CTO method. Various fault scenarios (0.0 V, and 1.4 V) have been tested under two case studies to show the impact of CTO. The cases are (without protection, and developed crowbar-based CTO. The DFIWG parameters are studied such as (P, V_{DC}, Q, ω_r) to show the impact of the proposed strategy on the machine performance.

MATLAB/Simulink is used to simulate the examined DFIWG to confirm the efficacy of the suggested strategy. To assess FRTC, the point of common coupling (PCC), where a bolted fault arises, is an important point. The system parameters are listed in Table 2 [37]. A detailed DFIWG model and its control system components are depicted in the Appendix.

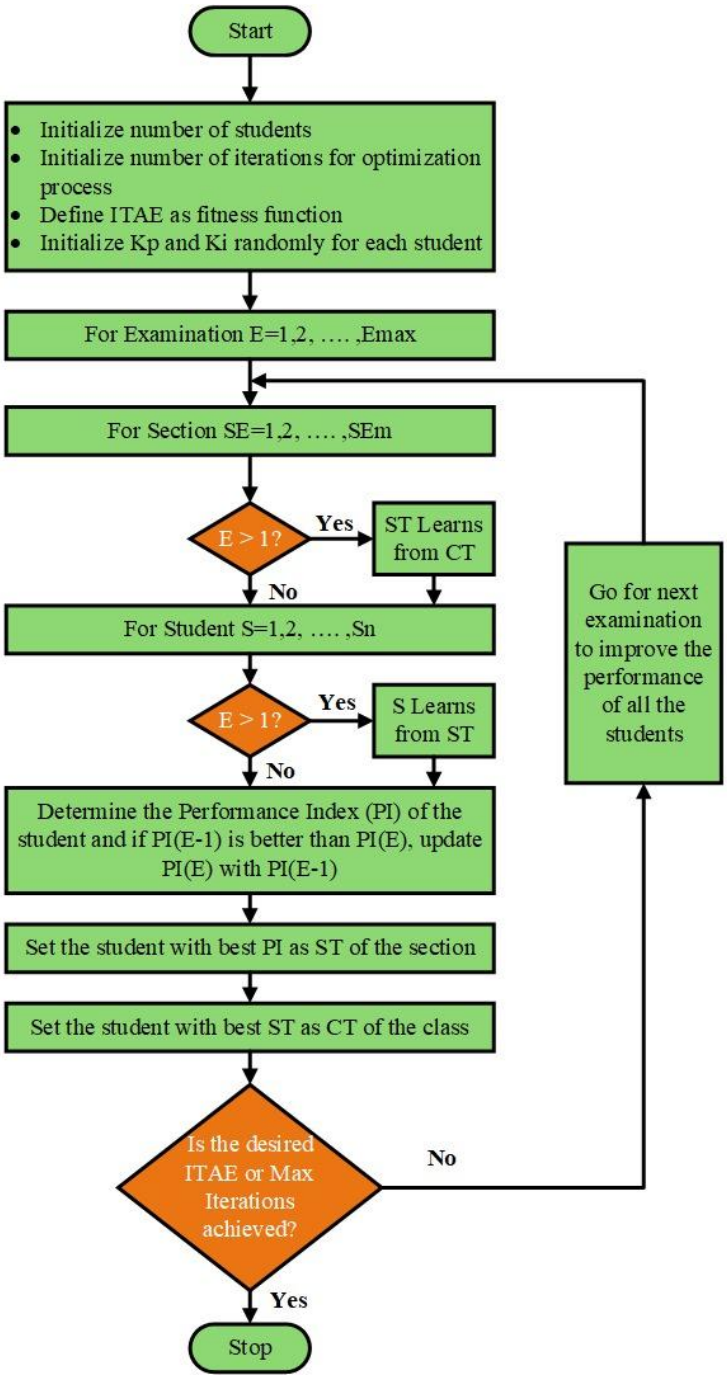

Fig. 2. Flowchart of CTO

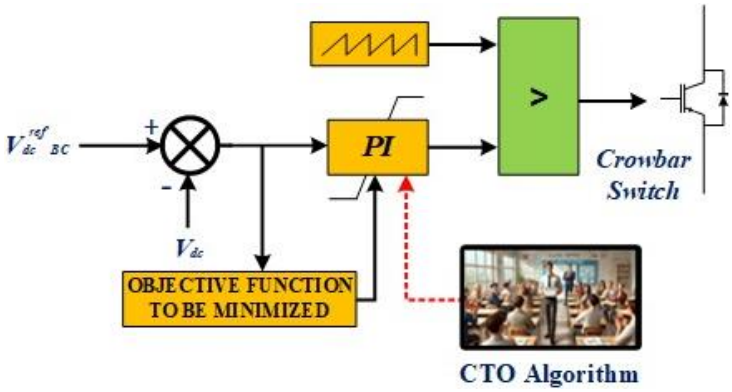

Fig. 3. Proposed control system of crowbar based on CTO-PI controller

Table 2. Simulated DFIWG data

DFIWG parameters	Value
Rated power	1.5 MW
Rated stator voltage	575 V
Rated frequency	60 Hz
V_{DC}	1150 V
Pole pairs	3
Stator resistance	0.023 pu
Rotor leakage inductance	0.16 pu
Mutual inductance	2.9 pu
Stator leakage inductance	0.18 pu
Rotor resistance	0.016 pu
Inertia constant	0.685

4.1. Case 1: 100% Voltage dip (VD)

The dynamic performance of DFIWG with a proposed crowbar and optimized controllers under a 100% VD at the PCC is evaluated in this part. The duration fault period is assumed to be 400 ms to test the efficacy of the proposed scheme. System voltage and current under 140% voltage swell is depicted in Fig. 4.

During fault, P decreases as seen in Fig. 5 (a), but an increase occurs in Q, V_{DC}, and ω_r as seen in Fig. 5 (b), (c), and (d) because of the drop happens in the grid voltage. To keep V_{DC} within the specified range, the braking chopper dissipates excess power as thermal energy as seen in Fig. 5 (c). The suggested method works well in this case where all parameters, including oscillations in ω_r, and overshoot of P, are damped. When Q is injected after a fault has been repaired and the DFIWG is still tied to the grid, FRT capability has been achieved. The observed simulated results show that the DFIWG continues to operate appropriately even in the face of serious failures. All DFIWG's fluctuations\variations for the cases under study are summarized and listed in Table 3.

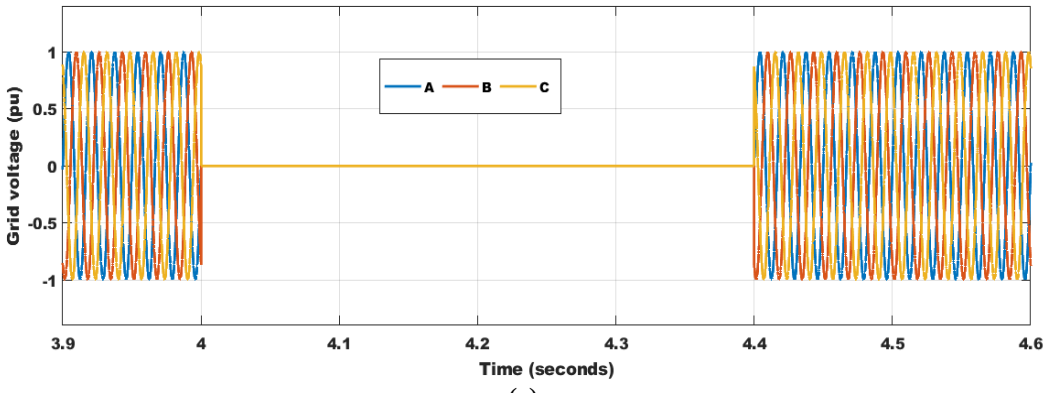

(a)

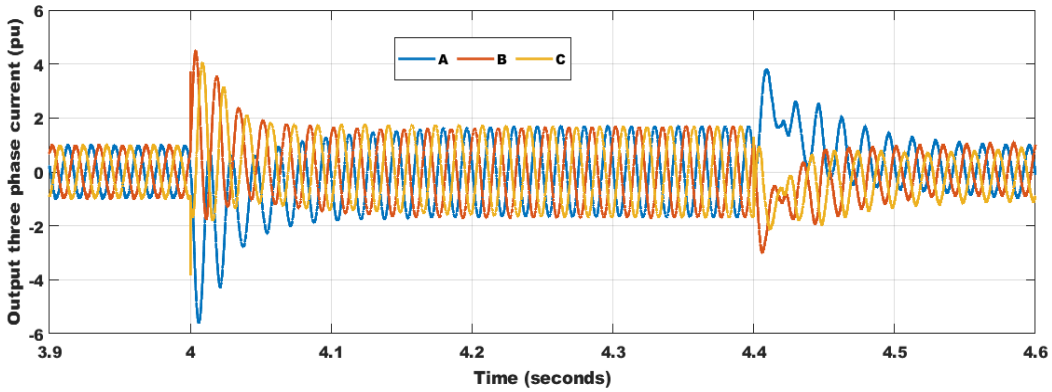

(b)

Fig. 4. System voltage and current under 100% VD

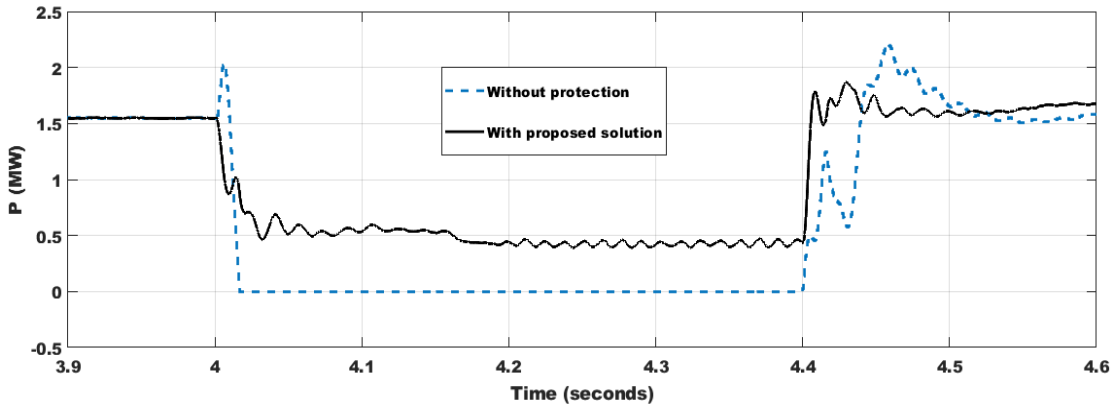

(a)

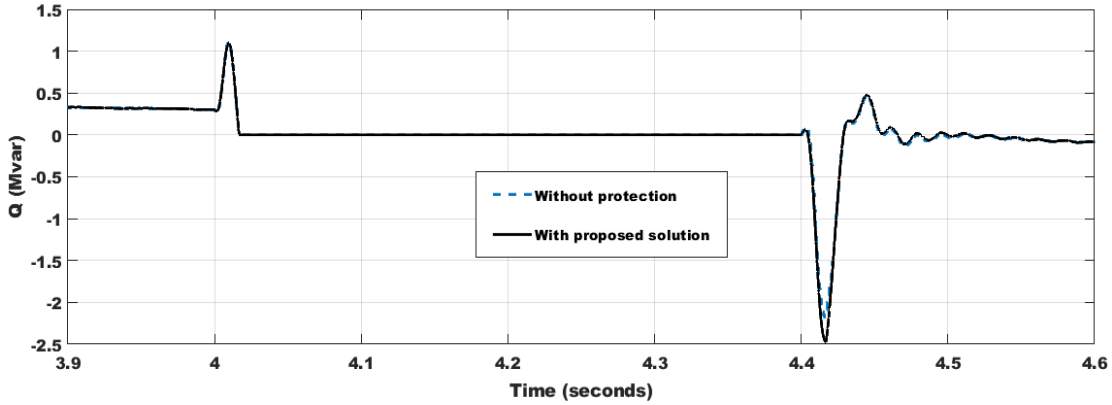

(b)

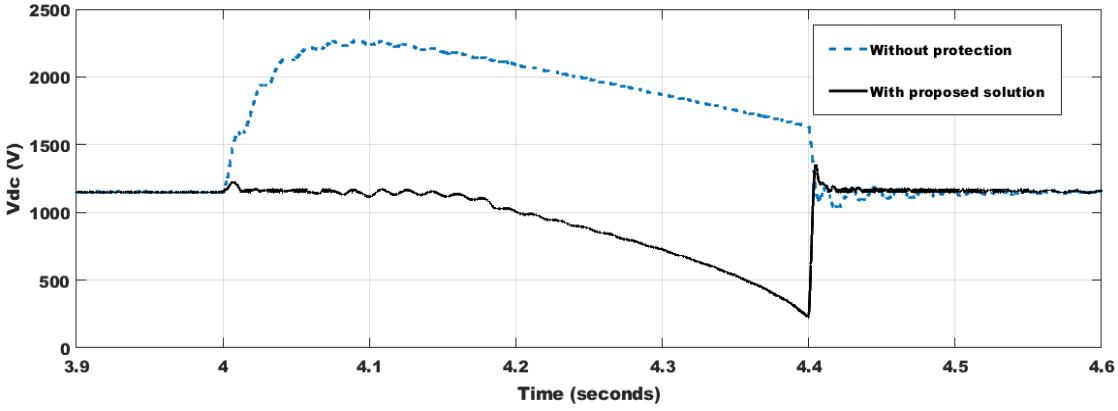

(c)

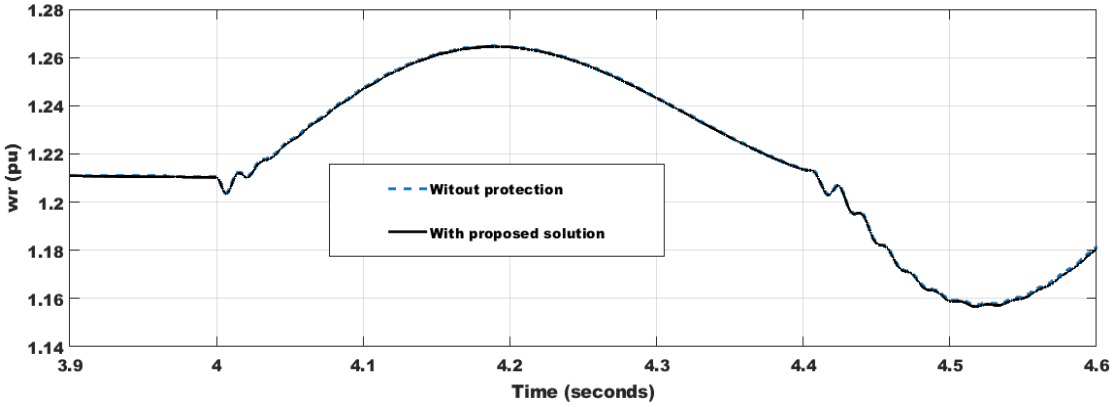

(d)

Fig. 5. DFIWG's parameters response as a result of 100% VD

4.2. Case 2: 140% VS

The dynamic performance of DFIWG with a proposed crowbar and optimized controllers under a 140% VS at the PCC is evaluated in this part. The duration fault period is assumed to be 400 ms to test the efficacy of the proposed scheme. System voltage and current under 140% voltage swell is depicted in Fig. 6.

During a fault, P decreases as seen in Fig. 7 (a), but an increase occurs in Q, V_{DC}, and ω_r as seen in Fig. 7 (b), (c), and (d) because of the increase that happens at the PCC. To keep V_{DC} within the specified range, the braking chopper dissipates excess power as thermal energy as seen in Fig. 7 (c). The suggested method works well in this case where all parameters, including oscillations in ω_r, and overshoot of P, are damped. When Q is injected after a fault has been repaired and the DFIWG is still tied to the grid, FRT capability has been achieved. The observed simulated results show that the DFIWG continues to operate appropriately even in the face of serious failures. DFIWG's fluctuations\variations for the cases under study are summarized and listed in Table 3.

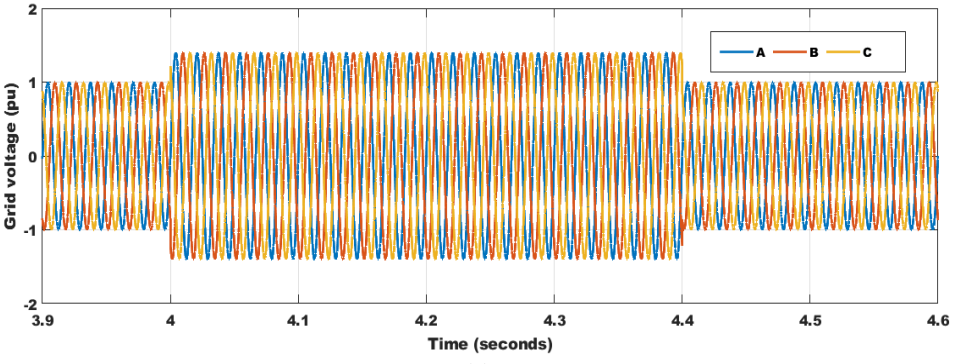

(a)

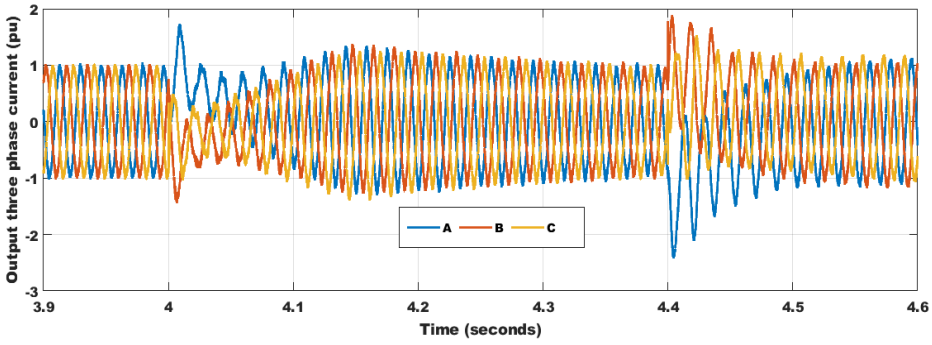

(b)

Fig. 6. System voltage and current under 140% voltage swell

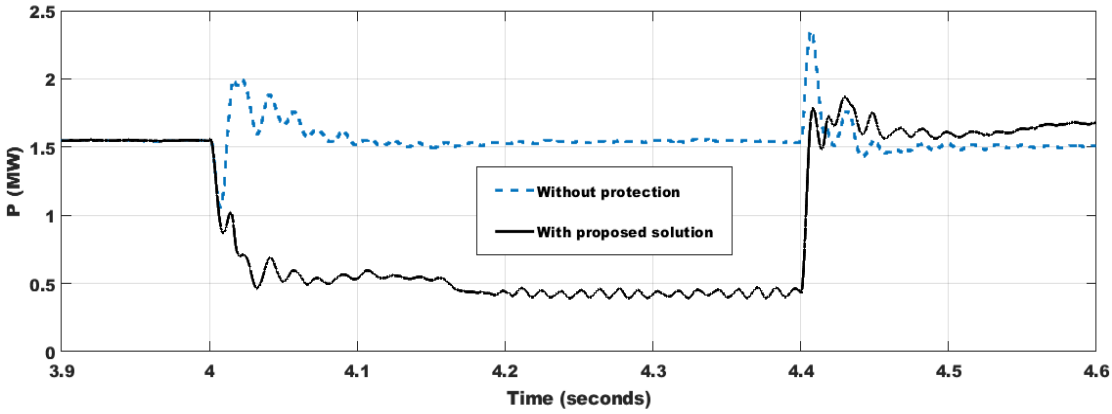

(a)

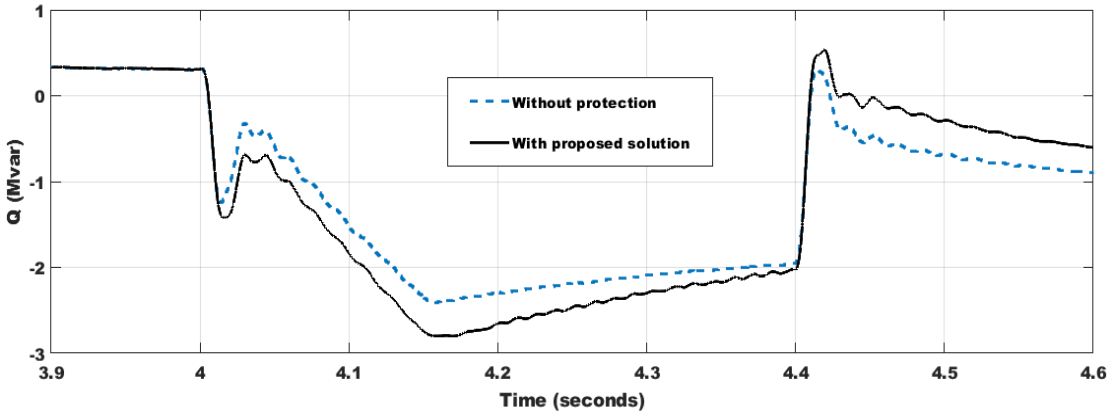

(b)

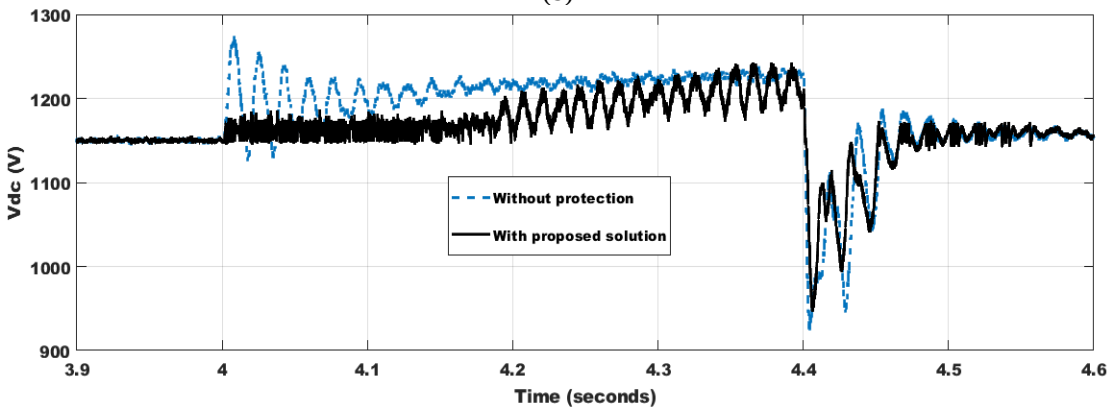

(c)

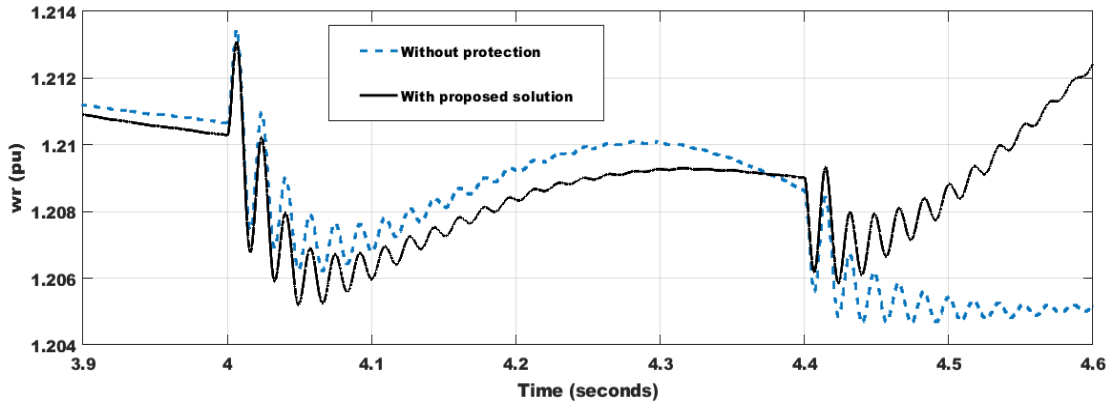

(d)

Fig. 7. DFIWG's parameters response as a result of 140% VS

Table 3. System response in studied cases

Parameters	100% VD		140% VS	
	Without Protection	With proposed Solution	Without Protection	With proposed Solution
p	≈ (0 → 2.1)	≈ (0.48 → 1.73)	≈ (1.1 → 2.4)	≈ (0.47 → 1.778)
Q	≈ (-2.5 → 1.1)	≈ (-2.5 → 1.1)	≈ (-2.4 → 0.37)	≈ (-2.8 → 0.37)
V_{DC}	≈ (1030 → 2370)	≈ (500 → 1170)	≈ (930 → 1280)	≈ (950 → 1200)
ω_r	≈ (1.157 → 1.263)	≈ (1.157 → 1.263)	≈ (1.205 → 1.2134)	≈ (1.2054 → 1.2121)

4.3. Power Quality Improvements

The DC offset of transient current appeared during the VD and VS, and the switching of RSC and GSC is the main cause of harmonic creation. This makes THD one of the most important essential traits. FFT analysis of the input current to the network during the examined cases is carried out. The results demonstrate the impact of the crowbar on the CTO. The FFT analysis is performed for the give-a-shot current to the network during the analyzed scenarios. As seen in Table 4, the THD is significantly lower in these CTO technique cases when compared to those without protection. According to the IEEE 1947–2003 standard limitations (THD level is less than 5%), the obtained findings show that the THD of the injected current to the grid is sufficient in the suggested method [56].

Table 4. Comparative performance for THD% in studied scenarios.

Studied Cases	THD without Protection	THD With the Proposed Solution	Reduction in THD
0 VD (pu)	5.07 %	1.35%	73.373 %
1.4 VS (pu)	7.83 %	2.73 %	65.134%

5. Conclusions

A devised crowbar control approach to improve the DFIWG's FRTC was provided in this research. The suggested strategy's structure, as stated in the introduction, enables it to get around the shortcomings of current approaches that have been documented in the literature. This is because it guarantees resilience in the event of grid failures, as evidenced by the results achieved. The CTO technique selects the best PI controller gains based on the OF. The CTO demonstrates its contribution to the crowbar's effective operation. The established method is based on straightforward calculations and is not affected by offsets or noise from sensors. The obtained findings demonstrated that, under the analyzed situations, the suggested approach maintained the DCLV below (1.1 pu). The controller parameters generated with CTO were found to have reduced rising, settling, and overshoot times. In every case under study, a decrease in THD was achieved within allowable bounds. Therefore, the suggested approach can work with the FRTC on a wind-driven DFIWG to meet grid code criteria.

Author Contribution: All authors contributed equally to the main contributor to this paper. All authors read and approved the final paper.

Data Availability: The data used to support the findings of this study are available at reasonable request from the corresponding author.

Conflicts of Interest: The authors declare that they have no conflicts of interest.

Acknowledgment: The authors extend their appreciation to Prince Sattam bin Abdulaziz University for funding this research work through the project number (PSAU/2024/01/29320).

Funding: The authors extend their appreciation to Prince Sattam bin Abdulaziz University for funding this research work through the project number (PSAU/2024/01/29320).

Appendix

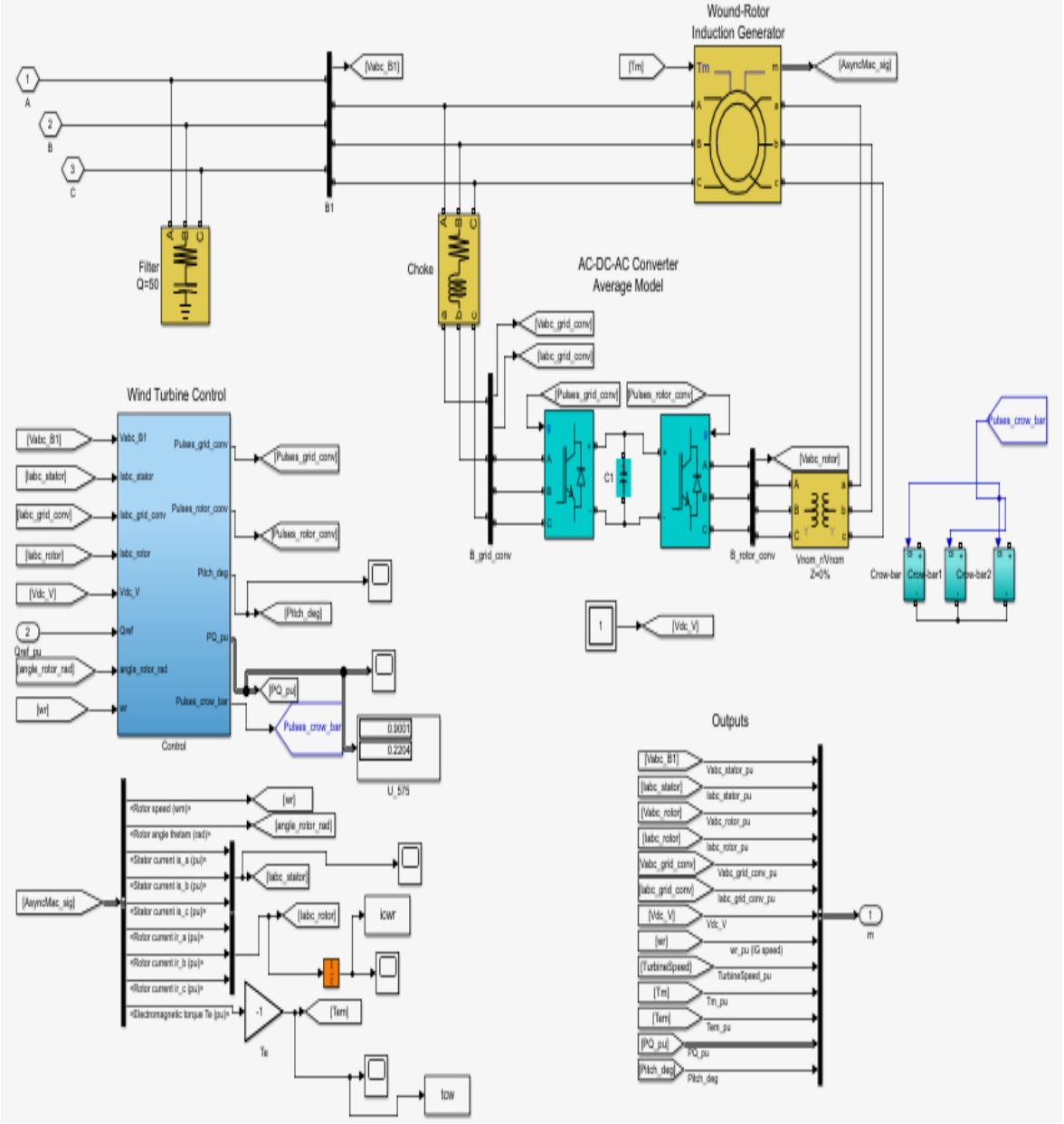

Fig. 8. Detailed DFIG MATLAB model

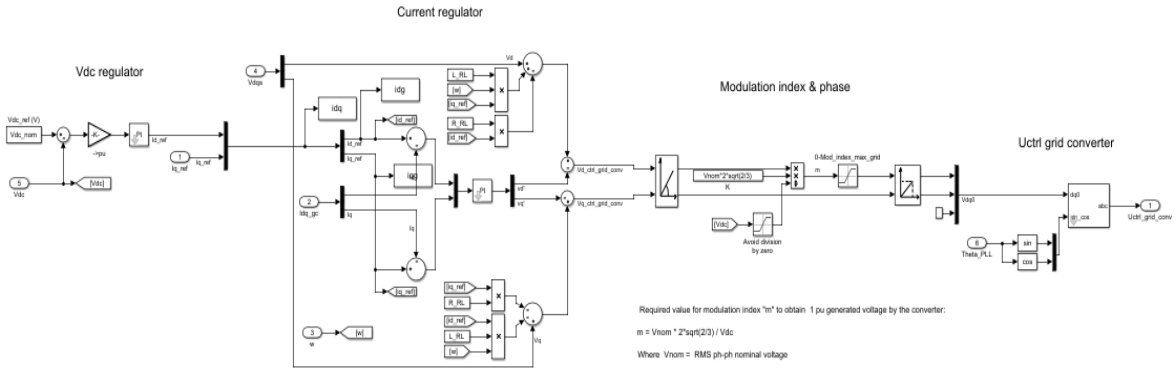

Fig. 9. GSC control model

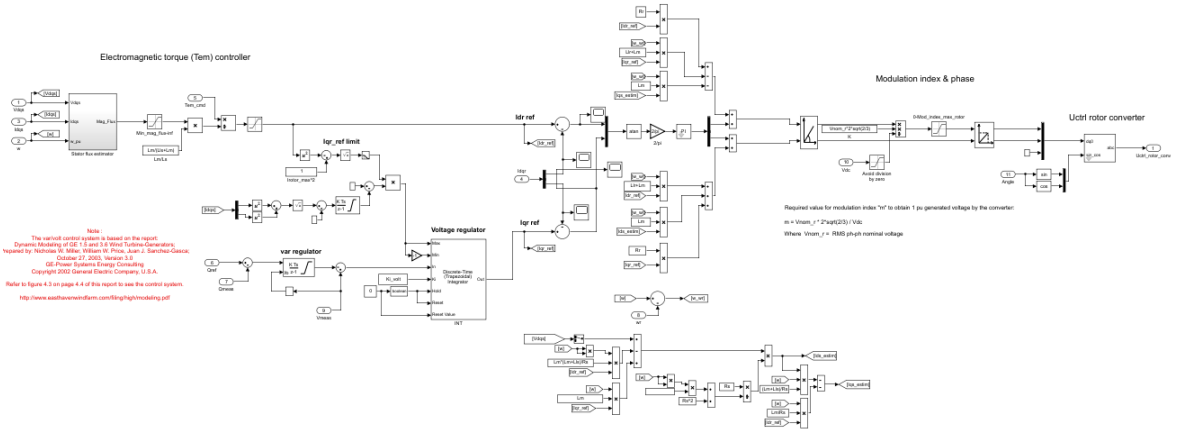

Fig. 10. RSC control model

References

[1] B. Krishna Ponukumati *et al*., "Evolving fault diagnosis scheme for unbalanced distribution network using fast normalized cross-correlation technique," *PLoS One*, vol. 19, no. 10, p. e0305407, 2024, https://doi.org/10.1371/journal.pone.0305407.

[2] B. S. Atia *et al*., "Applications of Kepler Algorithm-Based Controller for DC Chopper: Towards Stabilizing Wind Driven PMSGs under Nonstandard Voltages," *Sustainability* , vol. 16, no. 7, p. 2952, 2024, https://doi.org/10.3390/su16072952.

[3] A. M *et al*., "Prediction of Optimum Operating Parameters to Enhance the Performance of PEMFC Using Machine Learning Algorithms," *Energy Exploration & Exploitation*, 2024, https://doi.org/10.1177/01445987241290535.

[4] H. Abdelfattah *et al*., "Optimal controller design for reactor core power stabilization in a pressurized water reactor: Applications of gold rush algorithm," *PLoS One*, vol. 19, no. 1, p. e0296987, 2024, https://doi.org/10.1371/journal.pone.0296987.

[5] F. Menzri, T. Boutabba, I. Benlaloui, H. Bawayan, M. I. Mosaad, and M. M. Mahmoud, "Applications of hybrid SMC and FLC for augmentation of MPPT method in a wind-PV-battery configuration," *Wind Engineering*, vol. 48, no. 6, pp. 1186-1202, 2024, https://doi.org/10.1177/0309524X241254364.

[6] N. Benalia *et al*., "Enhancing electric vehicle charging performance through series-series topology resonance-coupled wireless power transfer," *PLoS One*, vol. 19, no. 3, p. e0300550, 2024, https://doi.org/10.1371/journal.pone.0300550.

[7] M. Awad *et al*., "A review of water electrolysis for green hydrogen generation considering PV/wind/hybrid/hydropower/geothermal/tidal and wave/biogas energy systems, economic analysis, and its application," *Alexandria Engineering Journal*, vol. 87, pp. 213–239, 2024, https://doi.org/10.1016/j.aej.2023.12.032.

[8] M. M. Mahmoud, M. Khalid Ratib, M. M. Aly, and A. M. M. Abdel-Rahim, "Wind-driven permanent magnet synchronous generators connected to a power grid: Existing perspective and future aspects," *Wind Engineering*, vol. 46, no. 1, pp. 189–199, 2022, https://doi.org/10.1177/0309524X211022728.

[9] M. M. Mahmoud, B. S. Atia, A. Y. Abdelaziz, and N. A. N. Aldin, "Dynamic Performance Assessment of PMSG and DFIG-Based WECS with the Support of Manta Ray Foraging Optimizer Considering MPPT, Pitch Control, and FRT Capability Issues," *Processes*, vol. 12, no. 10, p. 2723, 2022, https://doi.org/10.3390/pr10122723.

[10] S. R. K. Joga *et al*., "Applications of tunable-Q factor wavelet transform and AdaBoost classier for identification of high impedance faults: Towards the reliability of electrical distribution systems," *Energy Exploration & Exploitation*, vol. 42, no. 6, pp. 2017-2055, 2024, https://doi.org/10.1177/01445987241260949.

[11] N. F. Ibrahim, A. Alkuhayli, A. Beroual, U. Khaled, and M. M. Mahmoud, "Enhancing the Functionality of a Grid-Connected Photovoltaic System in a Distant Egyptian Region Using an Optimized Dynamic

Voltage Restorer : Application of Artificial Rabbits Optimization," *Sensors*, vol. 23, no. 16, p. 7146, 2023, https://doi.org/10.3390/s23167146.

[12] H. Miloudi *et al*., "Electromagnetic Compatibility Characterization of Start-Capacitor Single-Phase Induction Motor," *IEEE Access*, vol. 12, pp. 2313-2326, 2024, https://doi.org/10.1109/ACCESS.2023.3349018.

[13] M. M. Mahmoud, "Improved current control loops in wind side converter with the support of wild horse optimizer for enhancing the dynamic performance of PMSG-based wind generation system," *International Journal of Modelling and Simulation*, vol. 43, no. 6, pp. 952–966, 2023, https://doi.org/10.1080/02286203.2022.2139128.

[14] N. F. Ibrahim *et al*., "Operation of Grid-Connected PV System With ANN-Based MPPT and an Optimized LCL Filter Using GRG Algorithm for Enhanced Power Quality," *IEEE Access*, vol. 11, pp. 106859-106876, 2023, https://doi.org/10.1109/ACCESS.2023.3317980.

[15] N. F. Ibrahim *et al*., "Multiport Converter Utility Interface with a High-Frequency Link for Interfacing Clean Energy Sources (PV\Wind\Fuel Cell) and Battery to the Power System: Application of the HHA Algorithm," *Sustainability*, vol. 15, no. 18, p. 13716, 2023, https://doi.org/10.3390/su151813716.

[16] I. E. Maysse *et al*., "Nonlinear Observer-Based Controller Design for VSC-Based HVDC Transmission Systems Under Uncertainties," *IEEE Access*, vol. 11, pp. 124014-124030, 2023, https://doi.org/10.1109/ACCESS.2023.3330440.

[17] M. K. Döşoğlu, "Enhancement of LVRT Capability in DFIG-Based Wind Turbines with STATCOM and Supercapacitor," *Sustainability*, vol. 15, no. 3, p. 2529, 2023, https://doi.org/10.3390/su15032529.

[18] H. Mahvash and S. A. Taher, "A look-up table based approach for fault ride-through capability enhancement of a grid connected DFIG wind turbine," *Sustainable Energy, Grids and Networks*, vol. 10, pp. 128–140, 2017, https://doi.org/10.1016/j.segan.2016.12.001.

[19] H. Boudjemai *et al*., "Application of a Novel Synergetic Control for Optimal Power Extraction of a Small-Scale Wind Generation System with Variable Loads and Wind Speeds," *Symmetry*, vol. 15, no. 2, p. 369, 2023, https://doi.org/10.3390/sym15020369.

[20] M. M. Mahmoud *et al*., "Integration of Wind Systems with SVC and STATCOM during Various Events to Achieve FRT Capability and Voltage Stability: Towards the Reliability of Modern Power Systems," *International Journal of Energy Research*, vol. 2023, no. 1, pp. 1-28, 2023, https://doi.org/10.1155/2023/8738460.

[21] F. K. A. Lima, A. Luna, P. Rodriguez, E. H. Watanabe and F. Blaabjerg, "Rotor Voltage Dynamics in the Doubly Fed Induction Generator During Grid Faults," *IEEE Transactions on Power Electronics*, vol. 25, no. 1, pp. 118-130, 2010, https://doi.org/10.1109/TPEL.2009.2025651.

[22] S. R. Mosayyebi, S. H. Shahalami and H. Mojallali, "Fault Ride-Through Capability Improvement in a DFIG-Based Wind Turbine using Modified ADRC," *Protection and Control of Modern Power Systems*, vol. 7, no. 4, pp. 1-37, 2022, https://doi.org/10.1186/s41601-022-00272-9.

[23] S. Saeed, R. Asghar, F. Mehmood, H. Saleem, B. Azeem, and Z. Ullah, "Evaluating a Hybrid Circuit Topology for Fault-Ride through in DFIG-Based Wind Turbines," *Sensors*, vol. 22, no. 23, p. 9314, 2022, https://doi.org/10.3390/s22239314.

[24] L. V. Dai, "A Novel Protection Method to Enhance the Grid-Connected Capability of DFIG based on Wind Turbines," *IETE Journal of Research*, vol. 70, no. 2, pp. 2047-2063, 2023, https://doi.org/10.1080/03772063.2022.2163925.

[25] K. Gireeshma and S. Chandramohan, "Enhancing LVRT capability of DFIG using cooperative control of BTFCL and RPC," *Automatika*, vol. 64, no. 1, pp. 51–62, 2023, https://doi.org/10.1080/00051144.2022.2098108.

[26] K. Jayasawal and K. Thapa, "An Enhanced Low Voltage Ride-Through Control Scheme of a DIFG based WTG Using Crowbar and Braking Chopper," *Journal of the Institute of Engineering*, vol. 16, no. 1, pp. 61–67, 2021, https://doi.org/10.3126/jie.v16i1.36537.

[27] Z. Rafiee, S. S. Najafi, M. Rafiee, M. R. Aghamohammadi, and M. Pourgholi, "Optimized control of Coordinated Series Resistive Limiter and SMES for improving LVRT using TVC in DFIG-base wind

farm," *Physica C: Superconductivity and its Applications*, vol. 570, p. 1353607, 2020, https://doi.org/10.1016/j.physc.2020.1353607.

[28] N. F. Ibrahim *et al*., "A new adaptive MPPT technique using an improved INC algorithm supported by fuzzy self-tuning controller for a grid-linked photovoltaic system," *PLoS One*, vol. 18, no. 11, p. e0293613, 2023, https://doi.org/10.1371/journal.pone.0293613.

[29] M. M. Mahmoud *et al*., "Application of Whale Optimization Algorithm Based FOPI Controllers for STATCOM and UPQC to Mitigate Harmonics and Voltage Instability in Modern Distribution Power Grids," *Axioms*, vol. 12, no. 5, p. 420, 2023, https://doi.org/10.3390/axioms12050420.

[30] A. Chakraborty and T. Maity, "Integrated control algorithm for fast and accurate detection of the voltage sag with low voltage ride-through (LVRT) enhancement for doubly-fed induction generator (DFIG) based wind turbines," *Control Engineering Practice*, vol. 131, p. 105393, 2023, https://doi.org/10.1016/j.conengprac.2022.105393.

[31] P. S. Flannery and G. Venkataramanan, "A Fault Tolerant Doubly Fed Induction Generator Wind Turbine Using a Parallel Grid Side Rectifier and Series Grid Side Converter," *IEEE Transactions on Power Electronics*, vol. 23, no. 3, pp. 1126-1135, 2008, https://doi.org/10.1109/TPEL.2008.921179.

[32] A. E. Leon, J. M. Mauricio and J. A. Solsona, "Fault Ride-Through Enhancement of DFIG-Based Wind Generation Considering Unbalanced and Distorted Conditions," *IEEE Transactions on Energy Conversion*, vol. 27, no. 3, pp. 775-783, 2012, https://doi.org/10.1109/TEC.2012.2204756.

[33] R. Cardenas, R. Pena, S. Alepuz and G. Asher, "Overview of Control Systems for the Operation of DFIGs in Wind Energy Applications," *IEEE Transactions on Industrial Electronics*, vol. 60, no. 7, pp. 2776-2798, 2013, https://doi.org/10.1109/TIE.2013.2243372.

[34] N. A. N. Aldin, W. S. E. Abdellatif, Z. M. S. Elbarbary, A. I. Omar and M. M. Mahmoud, "Robust Speed Controller for PMSG Wind System Based on Harris Hawks Optimization via Wind Speed Estimation: A Real Case Study," *IEEE Access*, vol. 11, pp. 5929-5943, 2023, https://doi.org/10.1109/ACCESS.2023.3234996.

[35] M. Benbouzid, B. Beltran, Y. Amirat, G. Yao, J. Han, and H. Mangel, "Second-order sliding mode control for DFIG-based wind turbines fault ride-through capability enhancement," *ISA Transactions*, vol. 53, no. 3, pp. 827–833, 2014, https://doi.org/10.1016/j.isatra.2014.01.006.

[36] M. J. Hossain, T. K. Saha, N. Mithulananthan and H. R. Pota, "Control Strategies for Augmenting LVRT Capability of DFIGs in Interconnected Power Systems," *IEEE Transactions on Industrial Electronics*, vol. 60, no. 6, pp. 2510-2522, 2013, https://doi.org/10.1109/TIE.2012.2228141.

[37] S. Swain and P. K. Ray, "Short circuit fault analysis in a grid connected DFIG based wind energy system with active crowbar protection circuit for ridethrough capability and power quality improvement," *International Journal of Electrical Power & Energy Systems*, vol. 84, pp. 64–75, 2017, https://doi.org/10.1016/j.ijepes.2016.05.006.

[38] M. M. Mahmoud *et al*., "Evaluation and Comparison of Different Methods for Improving Fault Ride-Through Capability in Grid-Tied Permanent Magnet Synchronous Wind Generators," *International Transactions on Electrical Energy Systems*, vol. 2023, no. 1, pp. 1-22, 2023, https://doi.org/10.1155/2023/7717070.

[39] D. Zhu, X. Zou, S. Zhou, W. Dong, Y. Kang and J. Hu, "Feedforward Current References Control for DFIG-Based Wind Turbine to Improve Transient Control Performance During Grid Faults," *IEEE Transactions on Energy Conversion*, vol. 33, no. 2, pp. 670-681, 2018, https://doi.org/10.1109/TEC.2017.2779864.

[40] J. Mohammadi, S. Vaez-Zadeh, E. Ebrahimzadeh, and F. Blaabjerg, "Combined control method for grid-side converter of doubly fed induction generatorbased wind energy conversion systems," *IET Renewable Power Generation*, vol. 12, no. 8, pp. 943–952, 2018, https://doi.org/10.1049/iet-rpg.2017.0539.

[41] A. R. Nair, R. Bhattarai, M. Smith and S. Kamalasadan, "Parametrically Robust Identification Based Sensorless Control Approach for Doubly Fed Induction Generator," *IEEE Transactions on Industry Applications*, vol. 57, no. 1, pp. 1024-1034, 2021, https://doi.org/10.1109/TIA.2020.3035339.

[42] M. Firouzi, M. Nasiri, S. Mobayen, and G. B. Gharehpetian, "Sliding Mode Controller-Based BFCL for Fault Ride-Through Performance Enhancement of DFIG-Based Wind Turbines," *Complexity*, vol. 2020, no. 1, pp. 1-12, 2020, https://doi.org/10.1155/2020/1259539.

[43] M. R. Shafiee, H. S. Kartijkolaie, M. Firouzi, S. Mobayen, and A. Fekih, "A Dynamic Multi-Cell FCL to Improve the Fault Ride through Capability of DFIG-Based Wind Farms," *Energies*, vol. 13, no. 22, pp. 60–71, 2020, https://doi.org/10.3390/en13226071.

[44] B. Wadawa, Y. Errami, A. Obbadi, and S. Sahnoun, "Robustification of the H∞ controller combined with fuzzy logic and PI&PID-Fd for hybrid control of Wind Energy Conversion System Connected to the Power Grid Based on DFIG," *Energy Reports*, vol. 7, pp. 7539–7571, 2021, https://doi.org/10.1016/j.egyr.2021.10.120.

[45] H. Chojaa *et al*., "Nonlinear Control Strategies for Enhancing the Performance of DFIG-Based WECS under a Real Wind Profile," *Energies*, vol. 15, no. 18, p. 6650, 2022, https://doi.org/10.3390/en15186650.

[46] F. Shiravani, J. A. Cortajarena, P. Alkorta, and O. Barambones, "Generalized Predictive Control Scheme for a Wind Turbine System," *Sustainability*, vol. 14, no. 14, p. 8865, 2022, https://doi.org/10.3390/su14148865.

[47] M. B. Tuka and S. M. Endale, "Analysis of Doubly Fed Induction Generator-based wind turbine system for fault ride through capability investigations," *Wind Engineering*, vol. 47, no. 6, pp. 1132–1150, 2023, https://doi.org/10.1177/0309524X231186762.

[48] L. Simon, J. Ravishankar, and K. S. Swarup, "Coordinated reactive power and crow bar control for DFIG-based wind turbines for power oscillation damping," *Wind Engineering*, vol. 43, no. 2, pp. 95–113, 2019, https://doi.org/10.1177/0309524X18780385.

[49] A. Dendouga, A. Dendouga, and N. Essounbouli, "High performance of variable-pitch wind system based on a direct matrix converter-fed DFIG using third order sliding mode control," *Wind Engineering*, vol. 48, no. 3, pp. 325–348, 2024, https://doi.org/10.1177/0309524X231199435.

[50] A. M. A. Haidar, K. M. Muttaqi and M. T. Hagh, "A Coordinated Control Approach for DC link and Rotor Crowbars to Improve Fault Ride-Through of DFIG-Based Wind Turbine," *IEEE Transactions on Industry Applications*, vol. 53, no. 4, pp. 4073-4086, 2017, https://doi.org/10.1109/TIA.2017.2686341.

[51] Y. Ling, "A fault ride through scheme for doubly fed induction generator wind turbine," *Australian Journal of Electrical and Electronics Engineering*, vol. 15, no. 3, pp. 71–79, 2018, https://doi.org/10.1080/1448837X.2018.1525172.

[52] J. Yin, X. Huang, and W. Qian, "Analysis and research on short-circuit current characteristics and grid access faults of wind farms with multi-type fans," *Energy Reports*, vol. 11, pp. 1161–1170, 2024, https://doi.org/10.1016/j.egyr.2023.12.046.

[53] O. P. Mahela, N. Gupta, M. Khosravy and N. Patel, "Comprehensive Overview of Low Voltage Ride Through Methods of Grid Integrated Wind Generator," *IEEE Access*, vol. 7, pp. 99299-99326, 2019, https://doi.org/10.1109/ACCESS.2019.2930413.

[54] R. Hiremath and T. Moger, "Comprehensive review on low voltage ride through capability of wind turbine generators," *International Transactions on Electrical Energy Systems*, vol. 30, no. 10, pp. 1-39, 2020, https://doi.org/10.1002/2050-7038.12524.

[55] L. Yuan, K. Meng, J. Huang, Z. Yang Dong, W. Zhang, and X. Xie, "Development of HVRT and LVRT control strategy for pmsg-based wind turbine generators," *Energies*, vol. 13, no. 20, p. 5442, 2020, https://doi.org/10.3390/en13205442.

[56] M. M. Mahmoud, M. M. Aly, H. S. Salama, and A. M. M. Abdel-Rahim, "An internal parallel capacitor control strategy for DC-link voltage stabilization of PMSG-based wind turbine under various fault conditions," *Wind Engineering*, vol. 46, no. 3, pp. 983-992, 2021, https://doi.org/10.1177/0309524X211060684.